Electronic Supplementary Information

Rapid Microwave-Assisted Synthesis of Ni$_2$P Nanosheets from Black Phosphorus

Qicheng Zhang,[a] Junmei Liang,[e] Xuewen Hu,[a] An Cai,[a] Yuanzhi Zhu,[d] Wenchao Peng,[a] Yang Li,[a] Fengbao Zhang,[a] and Xiaobin Fan[a,b,c] *

[a] School of Chemical Engineering and Technology, State Key Laboratory of Chemical Engineering, Tianjin University, Tianjin 300072, China.

[b] Institute of Shaoxing, Tianjin University, Zhejiang 312300, China

[c] Haihe Laboratory of Sustainable Chemical Transformations, Tianjin 300192, China

[d] Faculty of Chemical Engineering, Kunming University of Science and Technology, The Higher Educational Key Laboratory for Phosphorus Chemical Engineering of Yunnan Province, Kunming University of Science and Technology, Kunming, 650500 China

[e] Beijing Institute of Metrology, Beijing, 100029, China

E-mail: xiaobinfan@tju.edu.cn

Experimental Section

Materials: Red phosphorus (99.999%), tin (Sn, 99.99%), tin (IV) iodide (SnI$_4$, 95%), propylene carbonate (PC, 99.7%, anhydrous), N, N-Dimethylformamide (DMF, 99%), p-nitrochlorobenzene (p-CNB, 99.5%) and nickel (II) chloride hexahydrate (NiCl$_2$·6H$_2$O, 98%) were provided by Aladdin Chemistry Co., Ltd. (Shanghai, China). Isopropanol (IPA, guaranteed reagent), and ethanol absolute (AR) were purchased from Yuanli Chemical Co., Ltd. (Tianjin, China). Tetra-n-butyl-ammonium bisulfate (TBA·HSO$_4$, 98%) was provided by Heowns Biochemical Technology Co., Ltd. (Tianjin, China). N-methyl pyrrolidone (NMP, 99.5%, extra dry) was purchased from Energy Chemical Co., Ltd. (Shanghai, China).

Synthesis of Bulk BP: The BP crystals are made by the chemical vapor transport (CVT) method of Nilges.[1] In brief, 500 mg of red phosphorus, 20 mg of Sn, and 10 mg of SnI$_4$ were loaded into a 10 cm long quartz tube in a glove box. The outer diameter of the quartz tube is 2.0 cm, and the wall thickness is 0.2 cm. The quartz tube was evacuated, sealed and placed horizontally in a tube furnace. Please note that the raw material is located at the hot end. The CVT process used the temperature profile described by Nilges.[1] The prepared bulk BP is stored in an inert atmosphere.

Synthesis of BP NSs: The BP NSs were prepared by an electrochemical cathodic exfoliation method.[2] This process uses a two-electrode system with bulk BP as the cathode and platinum foil as the anode, and a constant potential of –8 V is applied. The electrolyte used was a 0.1 M solution of TBA·HSO$_4$ in propylene carbonate (PC). During the entire exfoliation process, argon is continuously bubbled into the electrolyte solution to avoid oxidation of BP. Subsequently, BP was washed by centrifugation with anhydrous PC and isopropanol (IPA) at least 3 times. Thereafter, BP was dispersed in IPA and mild sonicated in an ice water bath for 15 minutes. The sonicated dispersion was centrifuged at 3000 rpm for 10 minutes to remove the unexfoliated part. The supernatant was filtered through a 0.22 µm pore size polyvinylidene fluoride (PVDF) membrane to obtain BP NSs and dispersed in extra dry NMP for later use.

Synthesis of Ni$_2$P NSs. Ni$_2$P NSs were synthesized by the microwave-assisted method. In brief, NiCl$_2$·6H$_2$O was dispersed in extra dry NMP to form a saturated solution (~1.1 mol/L). Subsequently, 10 mL of the saturated solution was added dropwise to 20 mL of a 1 mg/mL BP NSs/NMP solution under magnetic stirring at 500rpm, and the stirring was continued for more than 30 min. The feeding molar ratio of Ni:P is about 17.05, because excessive Ni precursor is necessary for the complete topochemical transformation of BP NSs. The mixture (30 mL) was moved to a 50 mL Schlenk flask and subjected to

microwave irradiation for 10 min by using a 2.45 GHz microwave chemical synthesizer (Shanghai Sineo, MAS-II) under an argon atmosphere, with magnetic stirring at 800 rpm and output power of 800 W. The sample was washed at least twice by suction filtration with ethanol absolute. The suction filtration process used polyvinylidene fluoride (PVDF) membranes with a pore size of 0.22 μm. Finally, the sample was sonicated for 30 min to disperse it in water and then vacuum freeze-dried at −50 °C for 48 h. Twenty milligram of BP NSs can be converted to 45 mg of Ni_2P NSs with a yield of about 47%. The loss may be attributed to washing step and the degradation of some BP NSs during the microwave process.

Characterization. Powder XRD analysis was performed using Bruker AXS D8-Focus with a Cu Kα radiation. SEM images were acquired using a Hitachi S-4800 at an accelerating voltage of 5 kV. TEM, HRTEM and EDS data with element mapping were obtained using a JEOL JEM-2100F at an accelerating voltage of 200 kV. The sample dispersions were dropped onto Cu grids with porous carbon film for TEM testing. Raman spectra were collected using a Horiba LabRAM HR Evolution with 532 nm laser excitation. The silicon peak of 520.7 cm^{-1} was used as the standard calibration Raman spectra. XPS experiments were performed using a Thermo Fisher Scientific K-Alpha+ instrument with a monochromatic Al Kα X-ray source. The binding energy is calibrated with C 1s of polluted carbon (284.8 eV is the correction value), and the vacuum condition is 5×10^{-8} Pa. The infrared heat maps are collected by a FLIR ONE Pro thermal imager with an accuracy of ±3°C or ±5% of the reading. The electromagnetic parameters were collected in a frequency range of 1–18 GHz by an Agilent PNA-N5244A network analyzer. The tested samples were pressed into a coaxial ring (outer diameter: 7.00 mm, inner diameter: 3.04 mm, thickness: 2 mm). UV–vis absorption spectra were collected by the UNICO UV-3802 spectrophotometer. Inductively coupled plasma optical emission spectrometer (ICP-OES) was measured by Thermo Fisher iCAP PRO.

Density functional theory (DFT) calculations. Spin-polarized DFT calculations were performed by using the Vienna ab initio Simulation Package (VASP).[3,4] The projector-augmented wave (PAW) method and Perdew-Burke-Ernzerhof (PBE) functional were used for the exchange-correlation energies.[5,6] The Brillouin zone was sampled by the 1×1×1 Monkhorst-Pack k-point mesh. The cutoff energy for the plane-wave basis was set to 400 eV. During the structure optimization, the convergence criterion of total energy was set to 10^{-5} eV, and atoms were relaxed until the force acting on each atom was less than 0.02 eV·$Å^{-1}$. A (2×2) supercell of 72 atoms for Ni_2P (111) were modeled. The cell dimensions are 13.530×13.530×18.321 Å. And a 15 Å vacuum space was used to minimize the interaction between slabs.

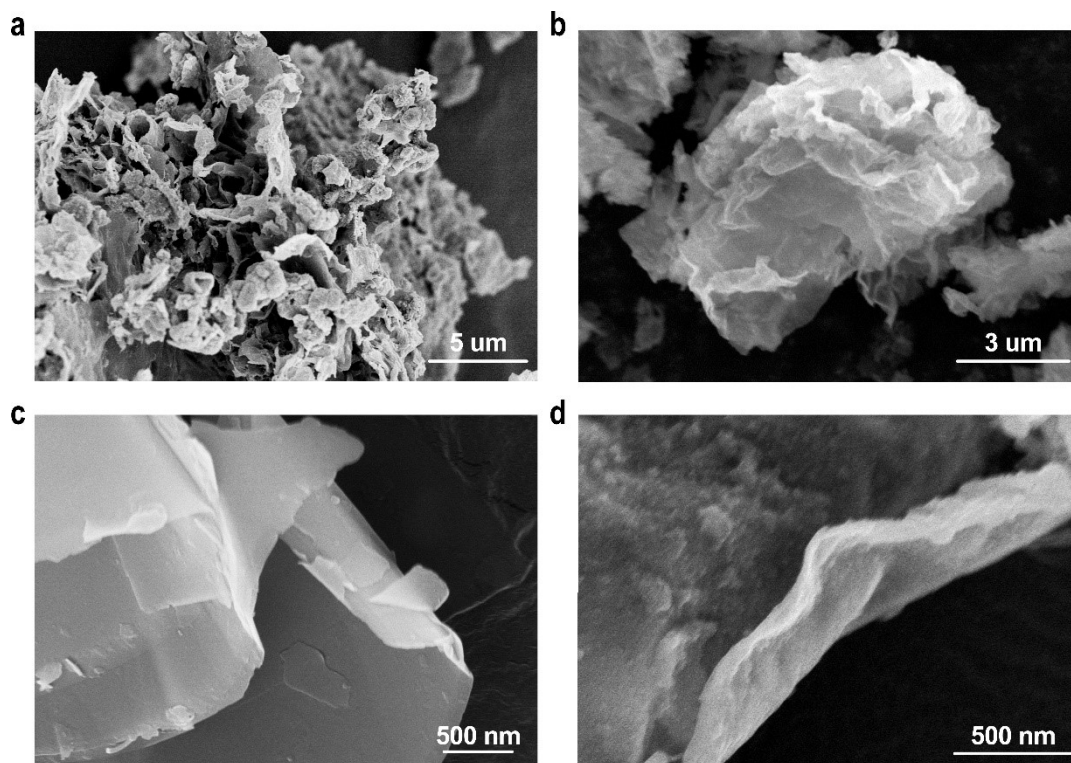**Supplementary Figures**
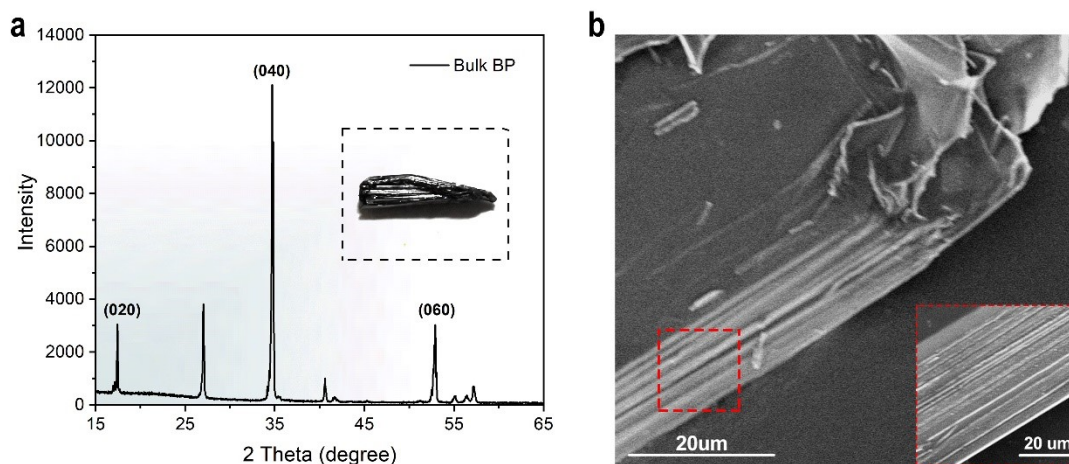
Fig. S1 (a) XRD pattern of bulk BP, and the insert is an optical image of the bulk BP. (**b**) SEM images of BP, and the insert is an enlarged cross-sectional of a bulk BP crystal.
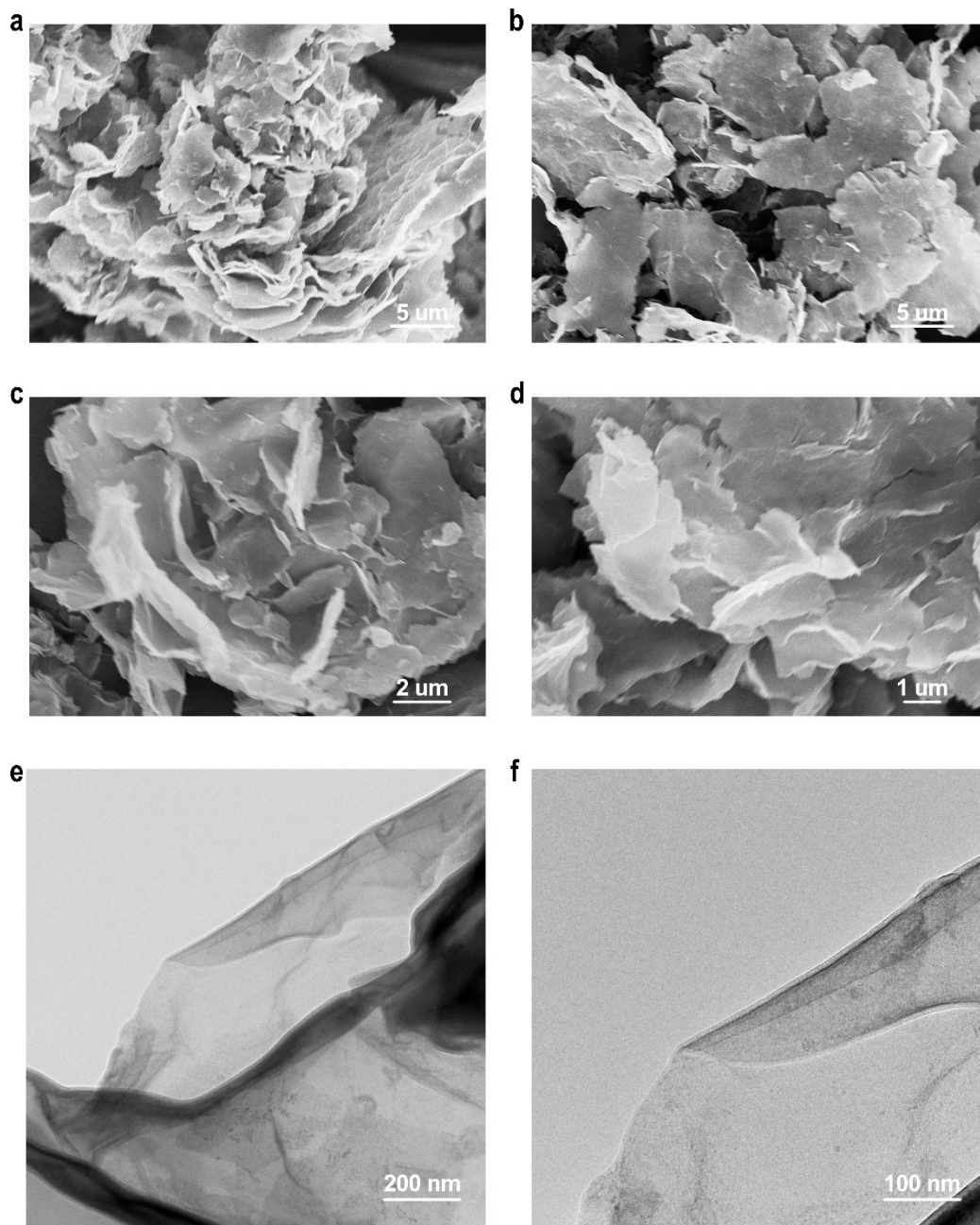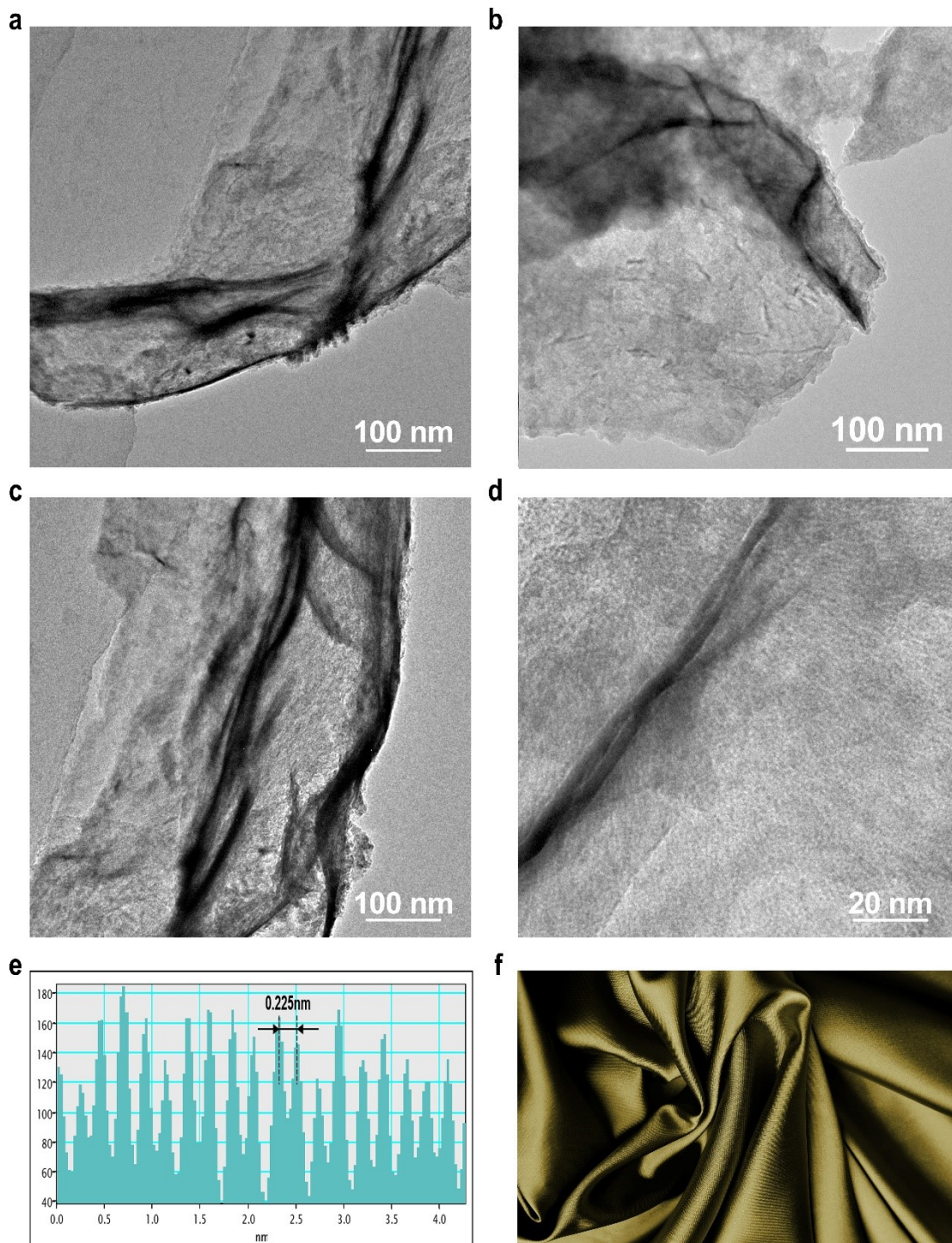
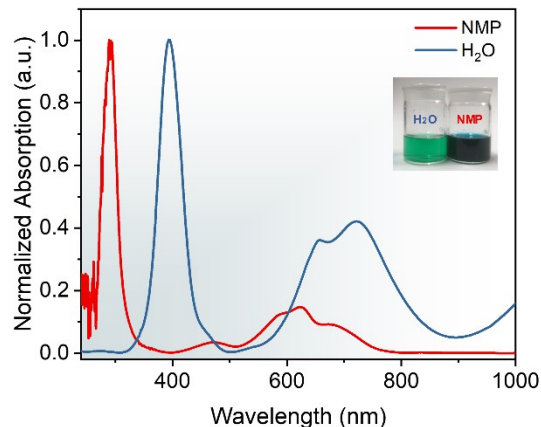**Fig. S2** (**a**)-(**d**) SEM and (**e**)-(**f**) TEM images of BP NSs.

Fig. S3 (**a**)-(**d**) SEM images of Ni$_2$P NSs.

**Fig. S4** (**a**)-(**d**) TEM images of Ni$_2$P NSs. (**e**) Intensity profile of the lattice fringes in Figure 2b. (**f**) A picture of satin.

Fig. S5 Normalized liquid UV-vis absorption spectra of Ni^{2+} in NMP and H_2O. The insets are optical photographs of $NiCl_2$ in water and NMP, respectively. As shown in Fig. S5, Ni^{2+} in NMP has three absorption peaks at 590, 625 and 685 nm, respectively, which are at shorter wavelength compared to Ni^{2+} in H2O. Meanwhile, the inset shows that Ni^{2+} in NMP appears blue due to absorption of orange light, while Ni^{2+} in H2O appears green due to absorption of red light. Given NMP is a strong field ligand, it will lead to a higher splitting energy of the d orbital of Ni^{2+} than H_2O. Therefore, the *d–d* electron transition of Ni^{2+} in NMP needs to absorb orange light with higher energy and shorter wavelength than red light.
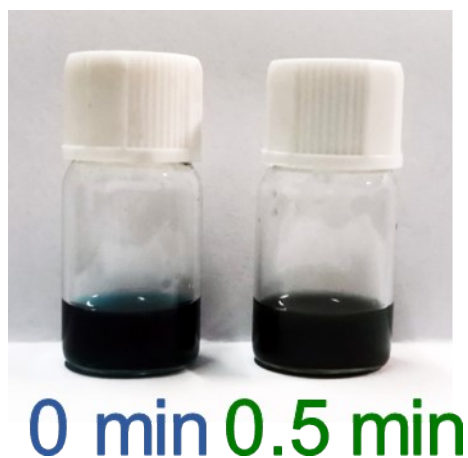
Fig. S6 Photographs of the mixture of BP NSs and saturated $NiCl_2 \cdot 6H_2O$ in NMP solution before and after microwave irradiation for 30 s.
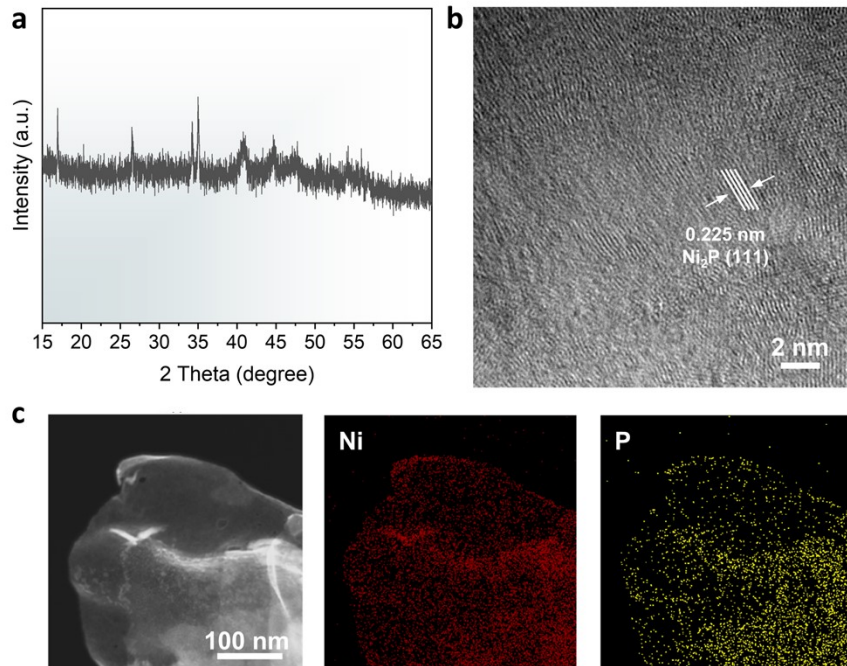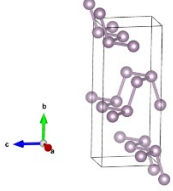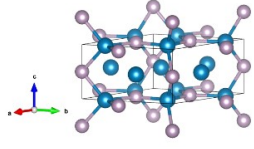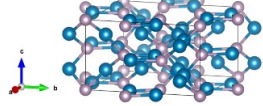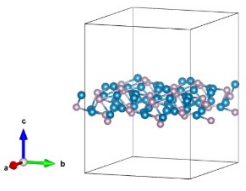
Fig. S7 (a) XRD pattern (b) TEM and (c) EDS mappings of the sample obtained by microwave irradiation in DMF. The experimental details are similar to the synthesis in NMP, just replace NMP with DMF. The XRD pattern confirmed the existence of BP and Ni_2P in the sample. The TEM images show that the samples are also nanosheets with uniform distribution of Ni and P. And there are both continuous Ni_2P lattices and amorphous regions. The amorphous regions may be unconverted BP or low-crystalline Ni_2P. These results confirm that microwave in DMF can also lead to Ni_2P phase, but phase conversion is incomplete due to the different physical properties between NMP and DMF.

Supplementary Table

Table S1. Feature parameter comparison of BP, Ni_2P, $Ni_{12}P_5$ and Ni_2P NSs.

	BP	Ni_2P	$Ni_{12}P_5$	Ni_2P NSs
Crystal System	Orthorhombic	Hexagonal	Tetragonal	Hexagonal
Crystal structure [a]				

XRD peaks [b]	2θ(°)	I(f)	(hkl)	d(Å)	2θ(°)	I(f)	(hkl)	d(Å)	2θ(°)	I(f)	(hkl)	d(Å)	2θ(°)	I(f)	(hkl)	d(Å)
	35.0	100	(111)	2.56	40.7	100	(111)	2.21	49.0	100	(312)	1.85	40.7	100	(111)	2.21
	26.5	55.5	(021)	3.36	44.6	59.6	(201)	2.03	47.0	62.8	(240)	1.93	44.6	59.6	(201)	2.03
	34.2	41.0	(040)	2.62	47.4	39.0	(210)	1.92	38.4	39.8	(112)	2.34	47.4	39.0	(210)	1.92

Raman peaks	362.50 cm^{-1} (A_g^1) 439.11 cm^{-1} (B_{2g}) 466.92 cm^{-1} (A_g^2)	n/a	n/a	n/a
Ni:P	0	2	2.4	1.92 [c]

[a] The Crystallography Open Database (COD) IDs of BP, Ni_2P and $Ni_{12}P_5$ are 9012486, 1537576 and 1537573, respectively. And the possible models of Ni_2P NSs simulations from DFT geometry optimization. The purple and blue spheres represent P and Ni atoms, respectively.
[b] The data are from Powder Diffraction File™ JCPDS No.76-1957, 74-1385 and 74-1381, corresponding to BP, Ni_2P and $Ni_{12}P_5$, respectively. The 2θ, I(f), (hkl) and d represents the diffraction angle, diffraction intensity, Miller symbol and interplanar spacing, respectively.
[c] The element content is measured by ICP-OES.

Supplemental References

1   M. Köpf, N. Eckstein, D. Pfister, C. Grotz, I. Krüger, M. Greiwe, T. Hansen, H. Kohlmann and T. Nilges, J. Cryst. Growth, 2014, 405, 6-10.

2   S. Yang, K. Zhang, A. G. Ricciardulli, P. Zhang, Z. Liao, M. R. Lohe, E. Zschech, P. W. M. Blom, W. Pisula, K. Muellen and X. Feng, Angew. Chem. Int. Edit., 2018, 57, 4677-4681.

3.   Kresse, G. and Furthmüller, J. Comput. Mater. Sci, 1996, 6, 15–50.

4.   Kresse, G. and Furthmüller, J. Phys. Rev. B., 1996, 54, 11169–11186.

5.   Blöchl, P. E. Phys. Rev. B, 1994, 50, 17953–17979.

6.   Perdew, J. P., Burke, K. and Ernzerhof, M. Phys. Rev. Lett., 1996, 77, 3865–3868.